DIRECTED ENERGY DEPOSITION

rtcoelho@sc.usp.br

PROCESSOS DE MANUFATURA ADITIVA

DIRECTED ENERGY DEPOSITION – Design for AM (DfAM)

Fig. 5.2 Comparison between CAD and actual part with direct metal laser sintering (DMLS) [9]

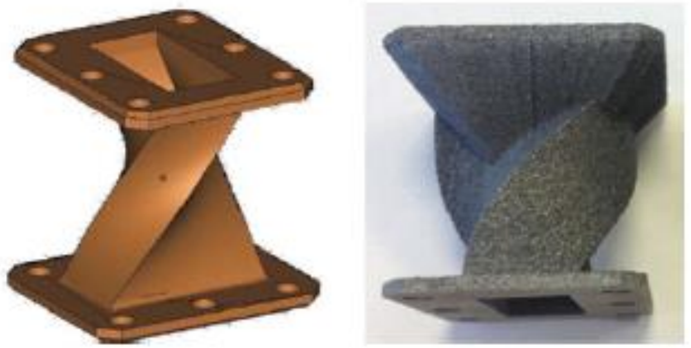

Conformal cooling

External complex shapes

Fig. 5.1 Calibration tool with conformal cooling channel designs [8]

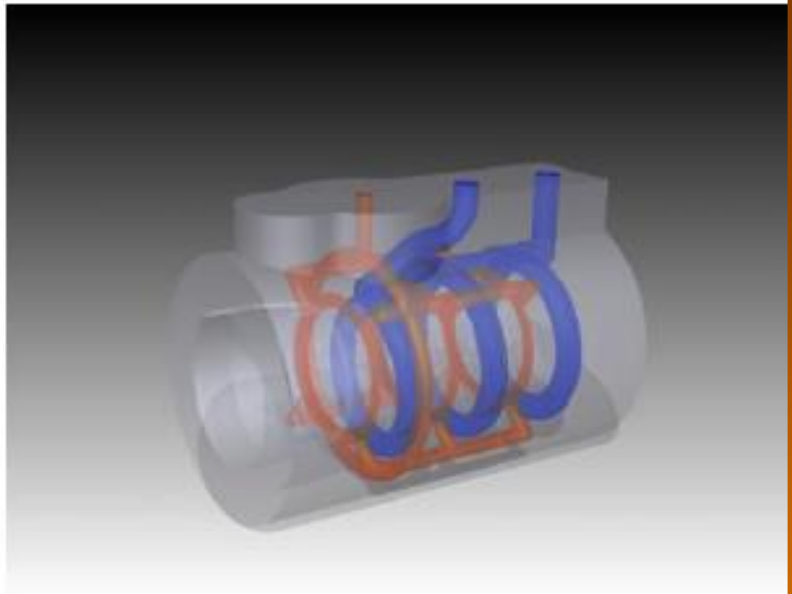

DIRECTED ENERGY DEPOSITION – Design for AM (DfAM)

Material properties

Table 5.1 Typical metal materials for powder bed fusion AM

Metal material	Modulus (GPa)	Ultimate strength (MPa)	Elongation (%)
Ti6Al4V [11, 12]	110–120	930–1020	10–14
CP-Ti [11]	–	570	21
316L Stainless steel [12, 13]	184–185	633–640	40
Maraging steel [12, 14]	160	1110	10–11
17-4PH Stainless steel [12, 14]	160–170	850–1300	10–25
Co-Cr-Mo [11, 12]	191–200	960–1100	20
IN625 [12, 13]	170–182	827–961	35
IN718 [12, 13]	166–170	994–1241	18
AlSi10Mg [12, 14, 15]	60–78	240–361	5–20

Tratamentos témicos

Name	Final heat treatment parameters
IN-718	1352 K/1 h + 991 K/8 h + 894 K/8 h
IN-625	1255 K/1 h
Hast-X	1422 K/1 h
Co-Cr	1464 K/1 h
Ti-6-4	1033 K/2 h
15-5PH	1339 K/3 min + 825 K/4 h
316L	1339 K/1 h
AlSi10Mg	802 K/5 h + 433 K/12 h

DIRECTED ENERGY DEPOSITION – Design for AM (DfAM)

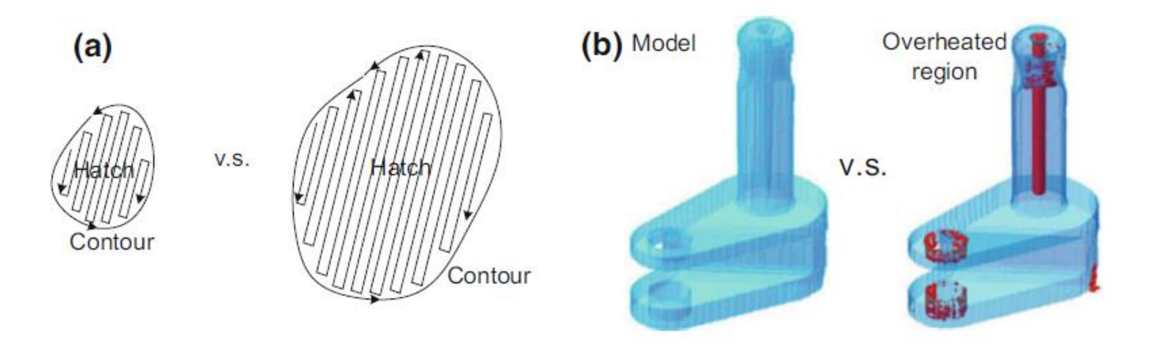

Fig. 5.8 Size-dependent characteristics of AM parts. a Material extrusion deposition pattern. b Laser sintering scanning vector length effect [42]

External surfaces

Estratégias de preenchimento

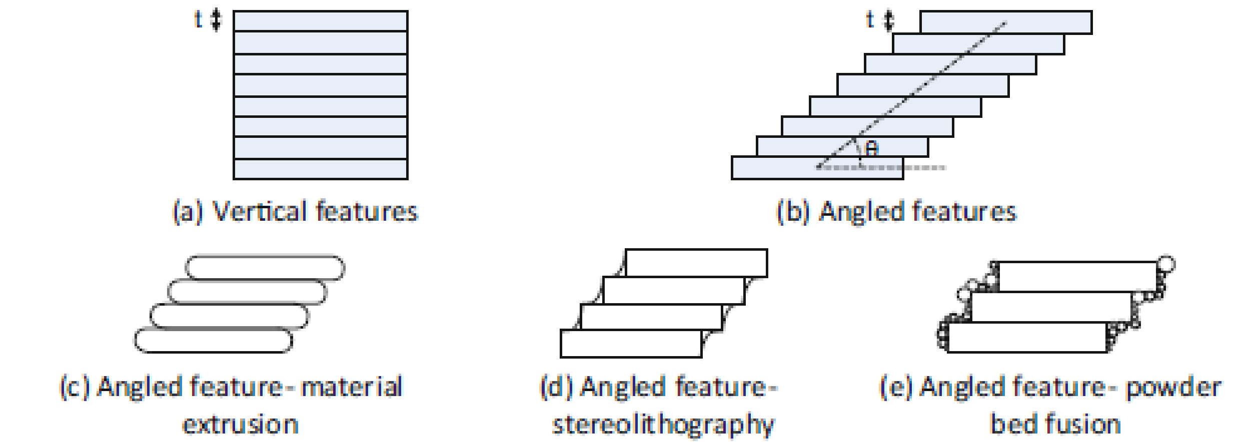

Fig. 5.5 Staircase effect of AM parts

DIRECTED ENERGY DEPOSITION – Design for AM (DfAM)

Need for support during construction in PBF

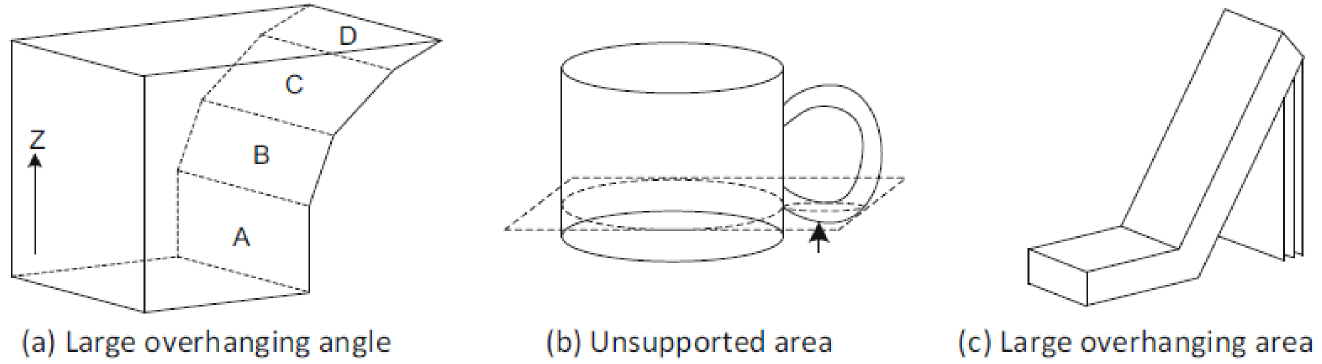

Fig. 5.11 Typical geometries that require support structures

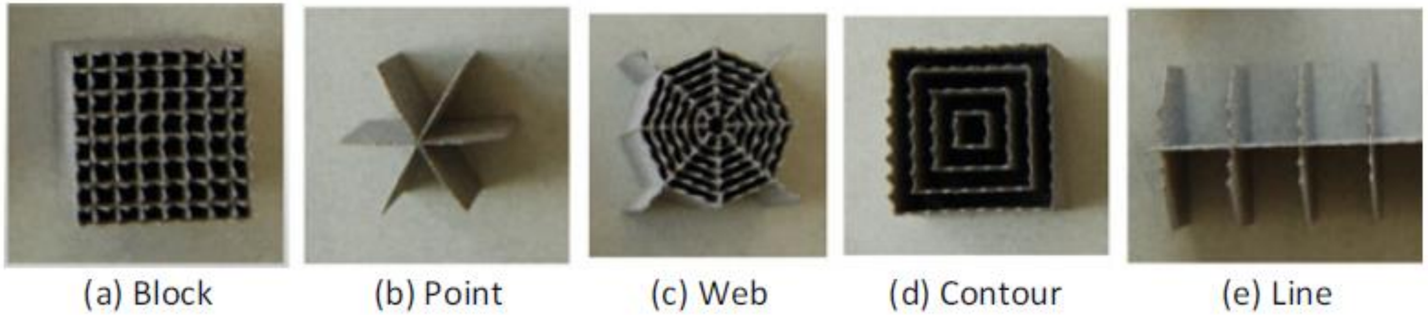

Fig. 5.13 Typical support geometries for metal powder bed fusion AM [27]

Need for support during construction in PBF

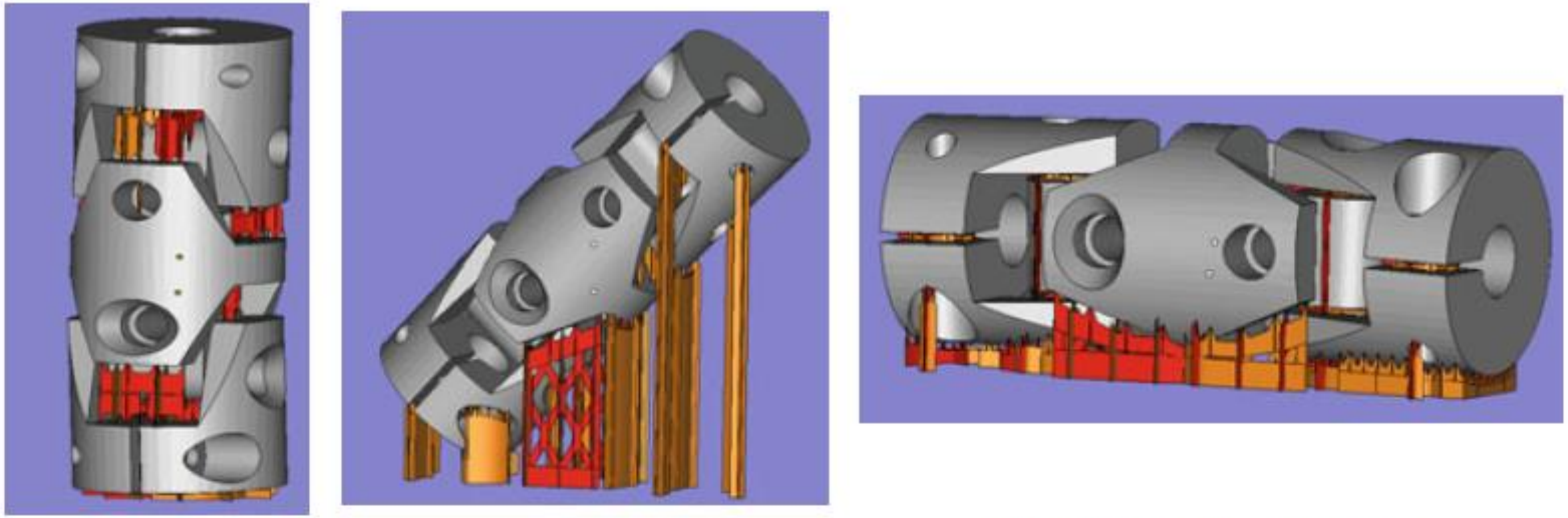

(a) Fewest support (b) Easy-to-remove support (c) Shortest fabrication time

Fig. 5.15 Support generation by Materialise Magics for a universal joint

Need for support during construction in PBF

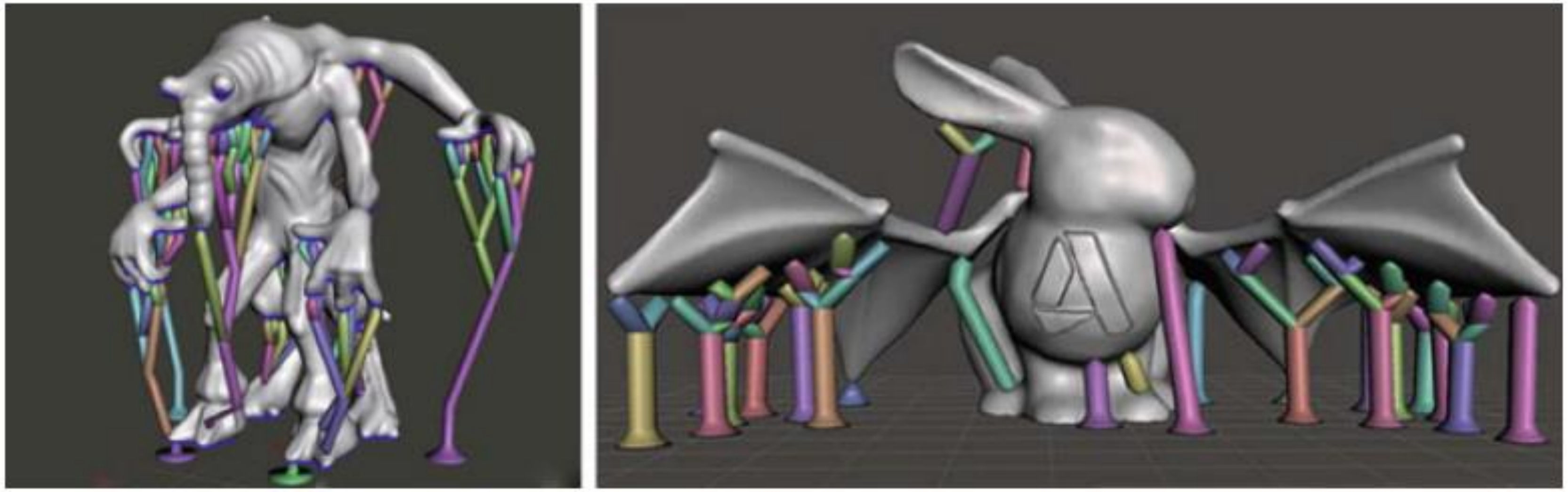

Fig. 5.20 Organic branch-like support generated by Autodesk Meshmixer [56]

DIRECTED ENERGY DEPOSITION – Design for AM (DfAM)

Topology Optimization

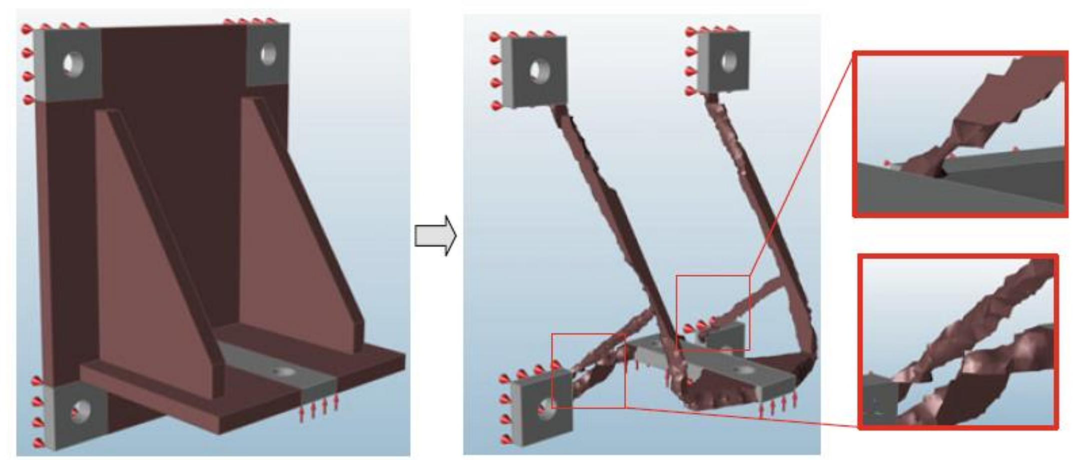

Fig. 5.46 Potentially non-manufacturable features generated by topology optimization

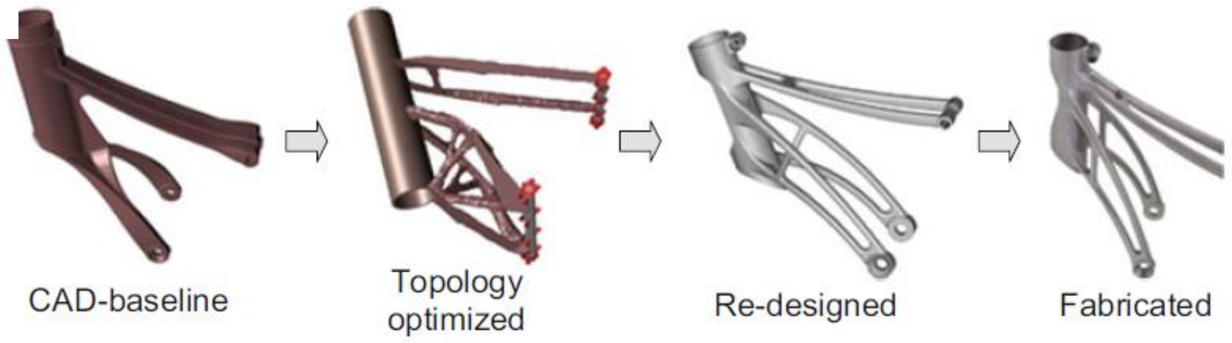

Fig. 5.47 Topology optimization as design reference [145]

DIRECTED ENERGY DEPOSITION – Design for AM (DfAM)

Benchmark design to test processes and machines

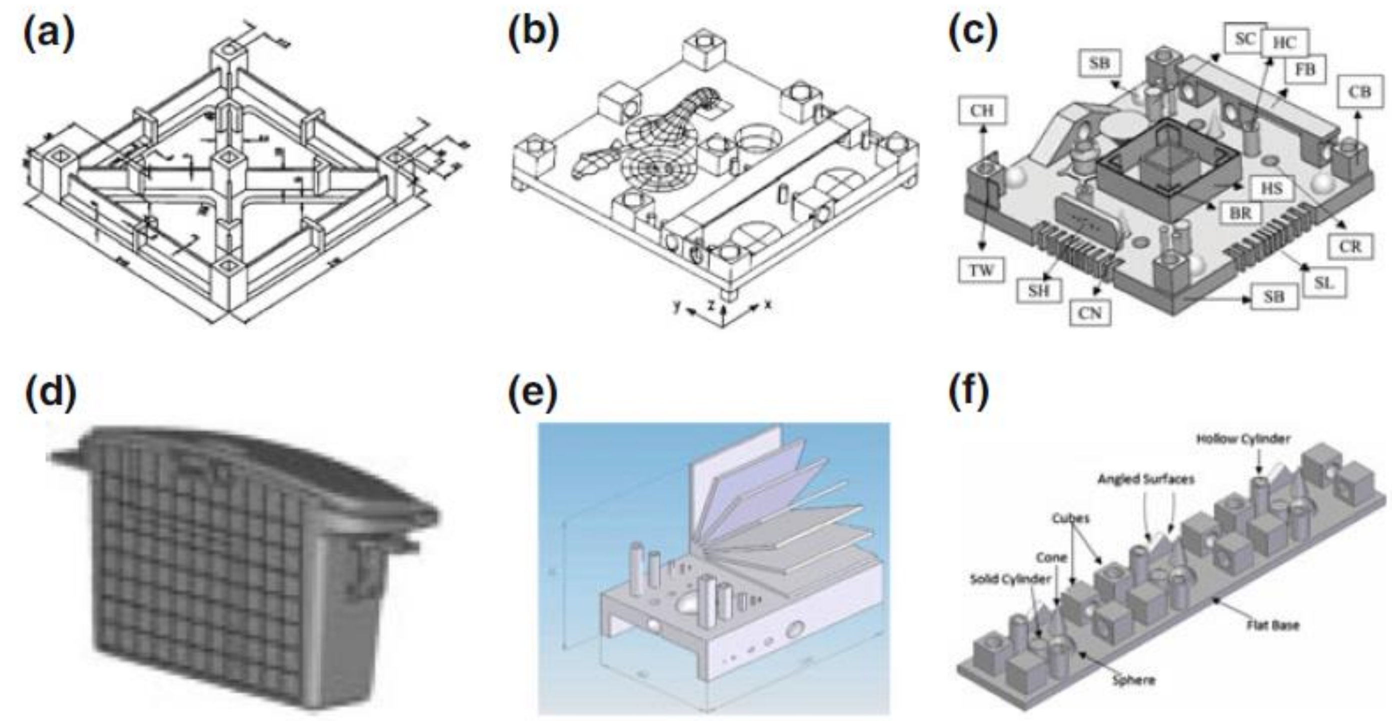

Fig. 5.7 Geometric benchmark design proposals. a 3D Systems [36]. b Childs and Juster [37]. c Mahesh et al. [38]. d Kim and Oh [39]. e Castillo [40]. f Fahad and Hopkinson [41]

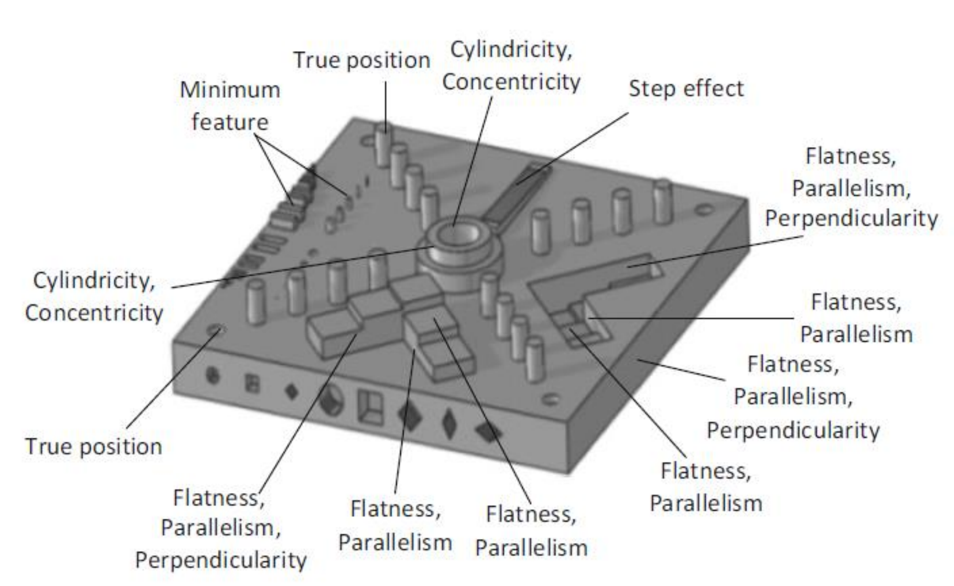

Post printing inspection and measurements

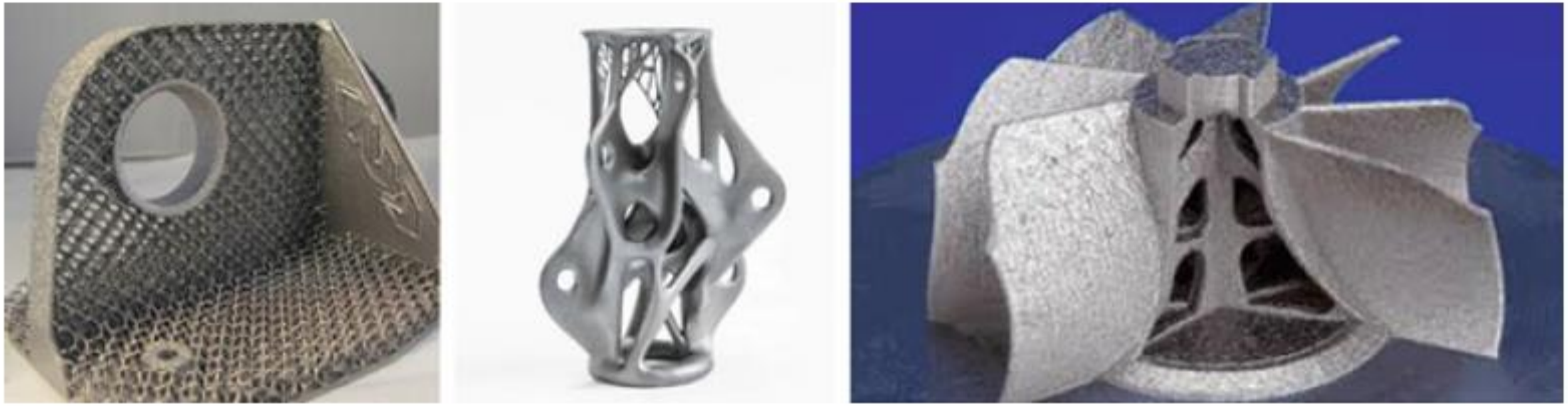

Fig. 5.10 Some freeform AM parts that are difficulty to inspect

DIRECTED ENERGY DEPOSITION – Material obtido

Material cerâmico – PBF

TABLE 5.1

Ceramic—Photocurable Polymer Systems in SLA

Ceramic Powder	Photocurable Polymer	References
Alumina (Al_2O_3)	Di-ethoxylated bisphenol a dimethacrylate (diacryl 101)	[5]
	Hexanediol diacrylate (HDDA)	[12]
	Diacryl 101 and HDDA	[13]
	Acrylamide	[4]
	Acrylic and silicon acrylate	[14]
	Acrylate	[9]
	Zirconate + 3% irgacure 184	[15]
Silica (SiO_2)	Acrylate	[3]
	Acrylamide	[4]
	acrylic and silicone acrylate	[16]
Lead zirconate titanate (PZT)	Acrylates (diacryl 101and HDDA) and epoxy-acrylates (SOMOS 6100)	[10,11]
Hydroxyapatite (HA)	SL5180 resin (Huntsman)	[9]
Barium titanate ($BaTiO_3$)	Hexanediol diacrylate (HDDA)	[17]
Titanium oxide (TiO_2)	Epoxy resin	[18]

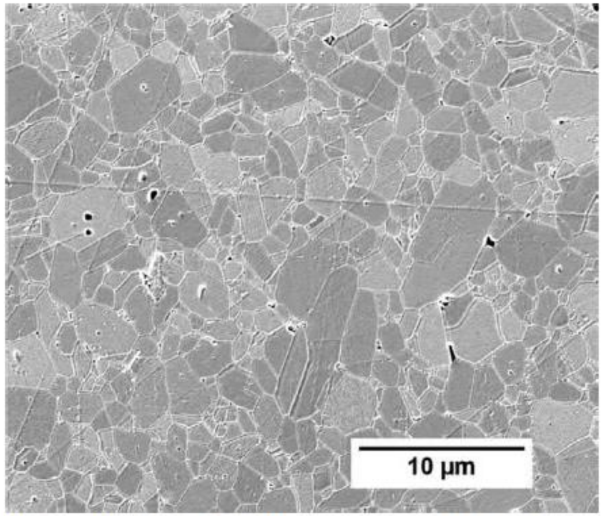

Fig. 3.22 SEM image showing a typical microstructure of the Al_2O_3 produced via the CODE process. *(Ghazanfari, A., Li, W., Leu, M., Watts, J., Hilmas, G., 2017. Int. J. Appl. Ceram. Technol. 14, 486. Open access.)*

DIRECTED ENERGY DEPOSITION – Material obtido

Material Ti6Al4V - PBF e DED

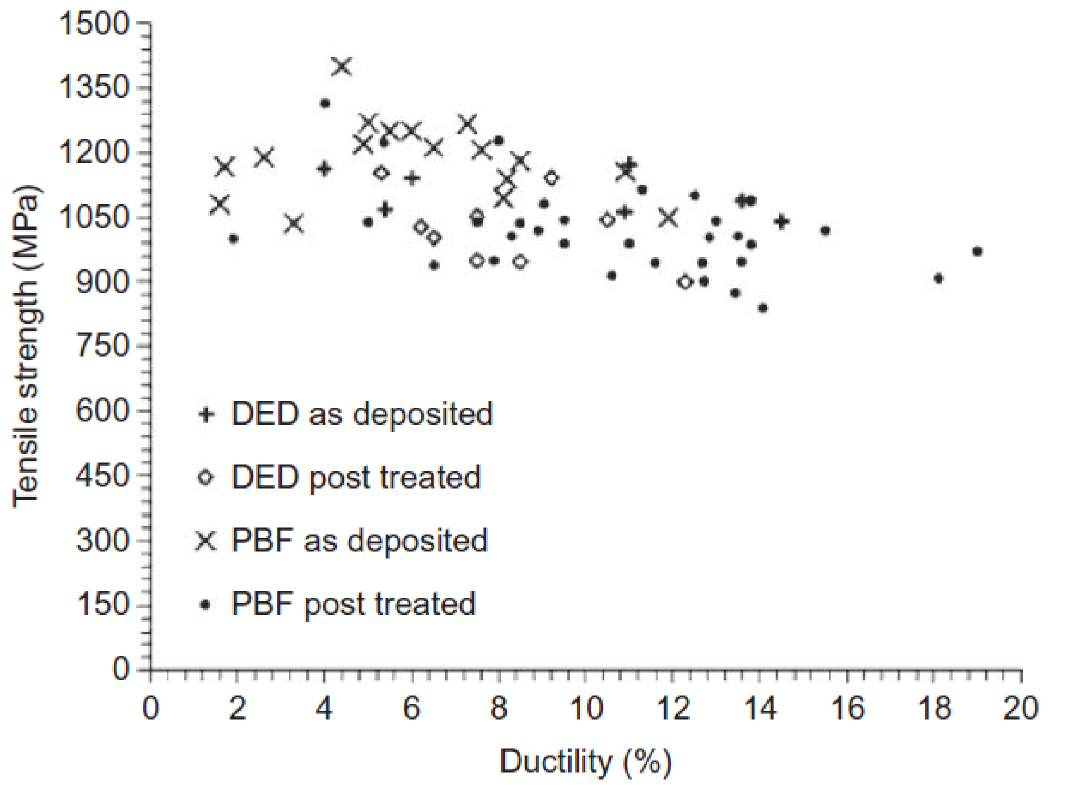

Fig. 3.3 Tensile strength versus ductility for as-deposited and heat-treated samples fabricated by directed energy deposition and powder-bed fusion. *(Data from Tables I, II, III, and IV. Beese, A.M., Carroll, B.E., 2016. JOM 68, 724. Open access.)*

PROCESSOS DE MANUFATURA ADITIVA

DIRECTED ENERGY DEPOSITION – Material obtido

Material Ti6Al4V - DED

Table 3.1 Mechanical properties of as-deposited Ti-6Al-4V fabricated by directed energy deposition.

	Laser			Mechanical properties					
Type	Power (W)	Scan rate (mm/s)	Linear heat input (J/mm)	Orientation	Elastic modulus (GPa)	Tensile yield (MPa)	Tensile strength (MPa)	Ductility (%)	References
Yb fiber	60–80	4	15–20	Longitudinal	–	–	1053 ± 49	–	Yao et al. (2015)
				Transverse	–	–	1035 ± 26	–	
CW Nd:YAG	130–190	8.5	15–22	–	–	950	–	~1	Zhang et al. (2001)
IPG fiber	470	16.7	28	Longitudinal	–	976 ± 24	1099 ± 2	4.9 ± 0.1	Yu et al. (2012)
TRUMPF DLD	1100–1200	12.5–14.2	77–96	Longitudinal	–	950 ± 2	1025 ± 10	12 ± 1	Qiu et al. (2015)
				Transverse	–	950 ± 2	1063 ± 2	5 ± 1	
IPG YLR–12000	2000	10.6	189	Longitudinal	–	960 ± 26	1063 ± 20	10.9 ± 1.4	Zhang et al. (2009)
				Transverse	–	958 ± 19	1064 ± 26	14 ± 1	
CO_2 laser	2400–2700	4–6	400–675	–	–	1070	1140	~6	Carroll et al. (2008)
CO_2 laser	300	0.61	490	Longitudinal	–	1105 ± 19	1163 ± 22	4 ± 1	Palmer and Beese (2015)
Optomec L850-R: low power	330	0.01	33,000	Longitudinal	–	1005	1103	4	Zhai et al. (2015)
Optomec L850-R: high power	780	0.013	60,000	Longitudinal	–	990	1042	7	
–	–	–	–	–	–	1069	1172	11	Keicher and Miller (1998)
Optomec	–	–	–	–	–	1077	973	11	http://www.optomec.com/3d-Printed-Metals/lens-Materials/ (2015). Accessed 15 November 2015

DIRECTED ENERGY DEPOSITION – Material obtido

Material Ti6Al4V - PBF

Table 3.2 Mechanical properties of as-deposited Ti-6Al-4V fabricated by power bed fusion.

	Laser deposition			Mechanical properties					
Type	Power (W)	Scan rate (mm/s)	Linear heat input (J/mm)	Orientation	Elastic modulus (GPa)	Tensile yield (MPa)	Tensile strength (MPa)	Ductility (%)	References
MTT 250 system	200	200	1	Longitudinal	–	910 ± 9.9	1035 ± 29	3.3 ± 0.76	21
Nd:YAG	95	125	0.76	–	94	1125	1250	6	29
–	160	600	0.27	Longitudinal	105 ± 5	1137 ± 20	1206 ± 8	7.6 ± 2	47
				Transverse	102 ± 7	962 ± 47	1166 ± 25	1.7 ± 0.3	
MTT SLM system	175	710	0.25	Longitudinal	–	1166 ± 6	1321 ± 6	2.0 ± 0.7 uniform	22
SMYb:YAG fiber	250	1600	0.16	Longitudinal	109.2 ± 3.1	1110 ± 9	1267 ± 5	7.28 ± 1.12	48
YAG	120–200	–	–	Longitudinal	110 ± 5	990 ± 5	1095 ± 10	8.1 ± 3	25
	–	–	–	Longitudinal	–	1040 ± 10	1140 ± 10	8.2 ± 0.3	
Nd:G	–	–	–	Longitudinal	118 ± 2.3	1100 ± 12	1211 ± 31	6.5 ± 0.6	26
Laser Cusing system	–	–	–	Transverse, unmachined	109.9	736	1051	11.9	33
				Transverse, machined	112.4	986	1155	10.9	
Yttrium fiber	–	–	–	Transverse		1008	1080	1.6	32
–	–	–	–	Longitudinal	–	1330	1400	4.4	31
Nd:YAG	150–200	–	–	Longitudinal	–	1070 ± 50	1250 ± 50	5.5 ± 1	23
				Transverse	–	1050 ± 40	1180 ± 30	8.5 ± 1.5	
EOS M270 system	–	–	–	Longitudinal	–	1195 ± 19	1269 ± 9	5 ± 0.5	24
				Transverse	–	1143 ± 30	1219 ± 20	4.89 ± 0.6	
EOS M270 system	–	–	–	Transverse	115	1005	1190	2.6	59
EOS	–	–	–	Longitudinal	110 ± 10	1060 ± 50	1230 ± 50	10 ± 2	60
				Transverse	110 ± 10	1070 ± 50	1200 ± 50	11 ± 3	

Beese, A.M., Carroll, B.E., 2016. JOM 68, 724. Open access.

DIRECTED ENERGY DEPOSITION – Material obtido

Material Ti6Al4V - DED + TT

Table 3.3 Mechanical properties of Ti-6Al-4V fabricated by directed energy deposition and subsequently heat treated.

		Mechanical properties				
Posttreatment	**Orientation**	**Elastic modulus (GPa)**	**Tensile yield (MPa)**	**Tensile strength (MPa)**	**Ductility (%)**	**References**
700–730°C, 2 h	Longitudinal	116	1066	1111	5.2	Yadroitsev et al. (2014)
	Transverse	112	832	832	0.8	
Low power, 760°C, 1 h, air cool	Longitudinal	–	1000	1073	9	Zhai et al. (2015)
High power, 760°C, 1 h, air cool	Longitudinal	–	991	1044	10	
950°C, 1 h, quench; 538°C, 4 h, air cool	Longitudinal	–	1052	1153	5.3	Amsterdam and Kool (2009)
	Transverse	–	1045	1141	9.2	
950°C, 1 h, air cool	–	–	975 ± 15	1053 ± 18	7.5 ± 1	Dinda et al. (2008)
950°C, 1 h, furnace cool	–	–	959 ± 12	1045 ± 16	10.5 ± 1	
950°C, 1 h, furnace cool	Longitudinal, unmachined	–	681 ± 35	750 ± 20	4.8 ± 1.6	Alcisto et al. (2011)
	Transverse, unmachined	–	637 ± 13	717 ± 12	3.4 ± 1.0	
	Longitudinal, machined	–	870 ± 37	953 ± 18	11.8 ± 1.3	
	Transverse, machined	–	830 ± 15	942 ± 13	9.7 ± 22	

DIRECTED ENERGY DEPOSITION – Material obtido

Material Ti6Al4V - PBF - Direção de impressão

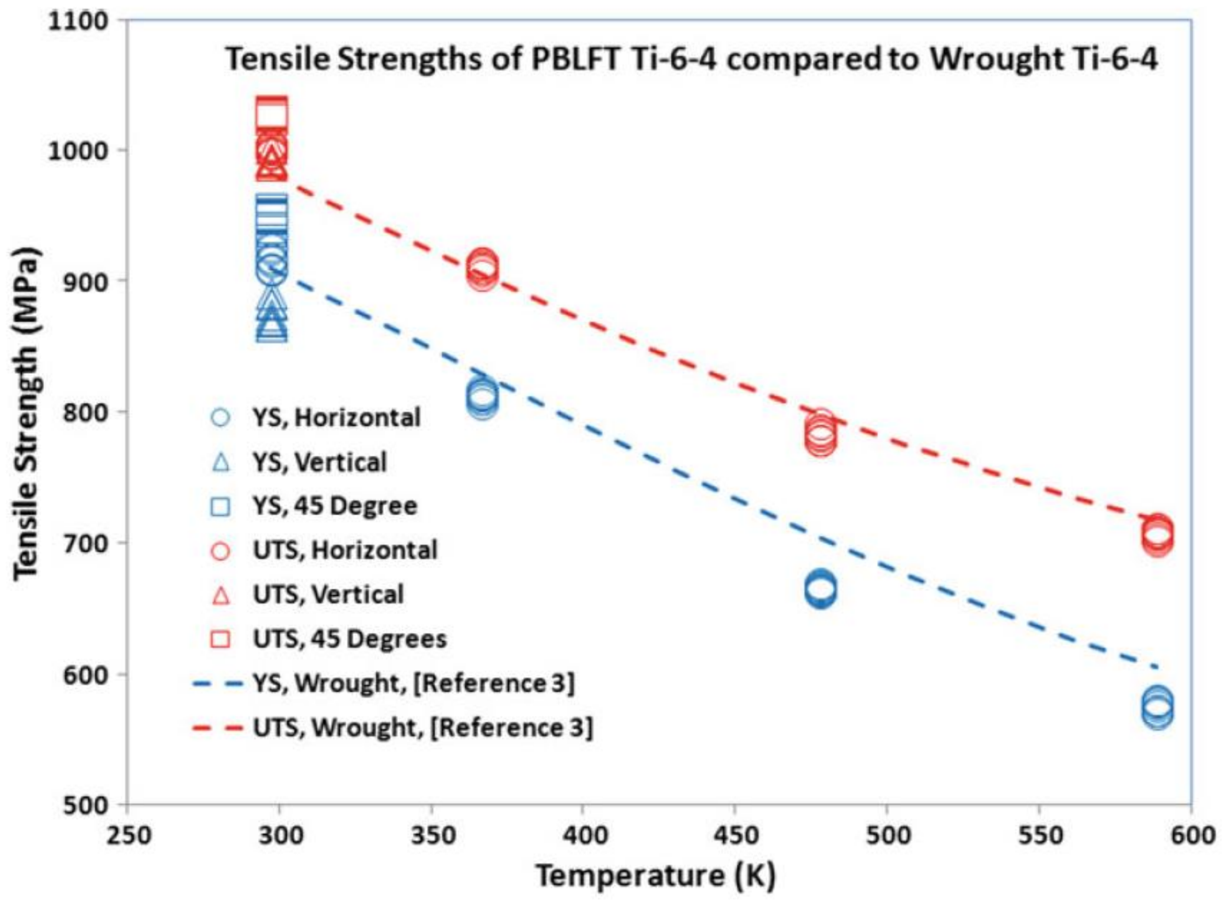

Fig. 3.3 Comparison of tensile strengths of PBLFT Ti-6-4 to wrought Ti-6-4

DIRECTED ENERGY DEPOSITION – Material obtido

Material Al 6061 - PBF

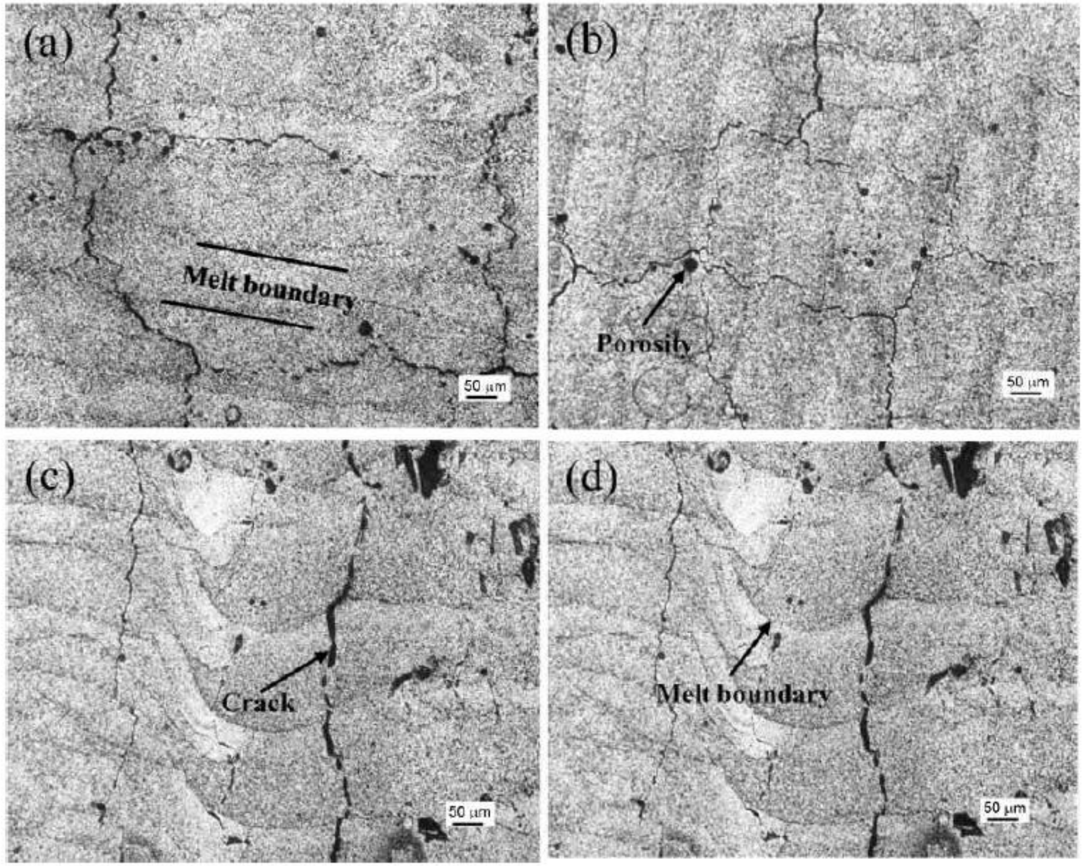

Fig. 3.8 Microstructure of AA6061 specimens fabricated on the unheated powder bed. (a) and (b) illustrate the *XY* plane (perpendicular to build direction). (c) and (d) show the *ZX* plane (build direction). Cracks, porosity, melt-pool, and melt-track banding are evident in the microstructure. *(Uddin, S.Z., Murr, L.E., Terrazas, C.A., Morton, P., Roberson, D.A., Wicker, R.B., 2018. Addit. Manuf. 22, 405. With kind permission of Elsevier.)*

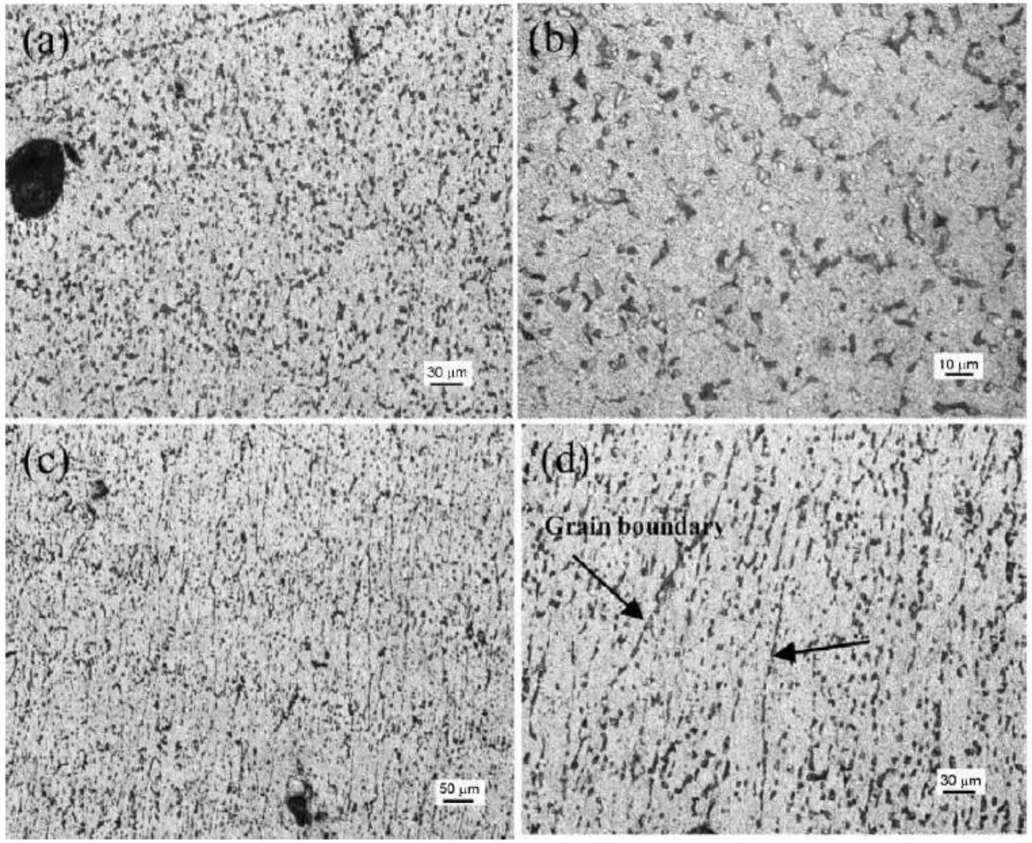

Fig. 3.9 Microstructure of AA6061 specimens fabricated on powder-bed heated to 500°C. (a) and (b) illustrate the *XY* plane (perpendicular to build direction). (c) and (d) show the *ZX* plane (build direction). Cracks, porosity, melt pool, and melt-track banding removed from the microstructure, and a columnar grain growth is observed in the build direction. *(Uddin, S.Z., Murr, L.E., Terrazas, C.A., Morton, P., Roberson, D.A., Wicker, R.B., 2018. Addit. Manuf. 22, 405. With kind permission of Elsevier.)*

DIRECTED ENERGY DEPOSITION – Material obtido

Material Al 6061 - PBF

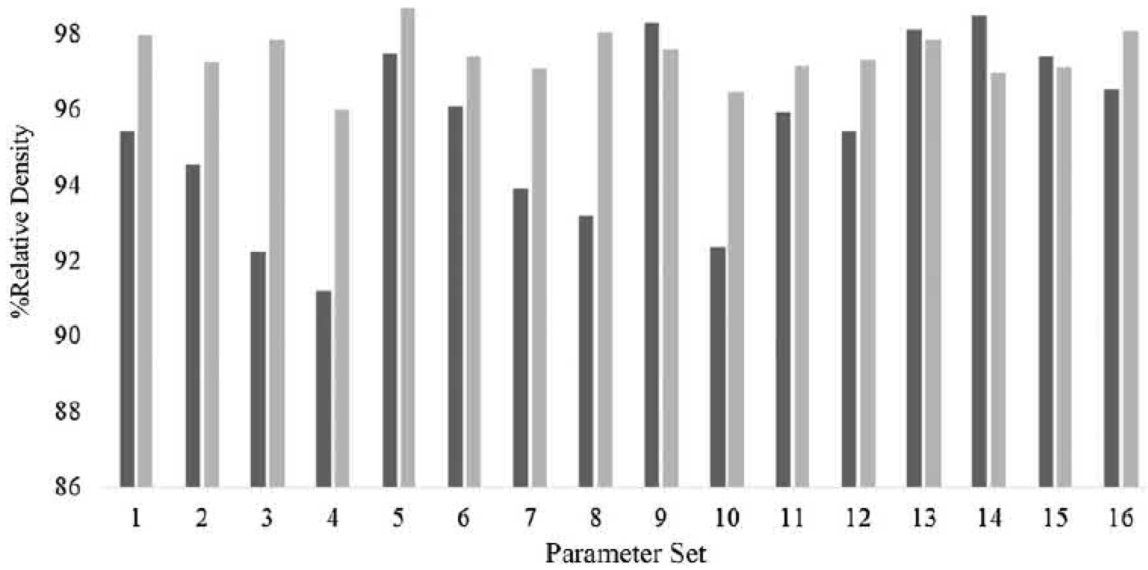

Parameter set	1	2	3	4	5	6	7	8	9	10	11	12	13	14	15	16
Laser Power (W)	350	400	450	500	300	400	450	500	350	400	450	500	350	400	450	500
Scanning Speed (mm/s)	1400	1600	1800	2000	1400	1600	1800	2000	1400	1600	1800	2000	1400	1600	1800	2000

Fig. 3.7 Relative density of AA6061 cube coupons fabricated using different laser power and scanning speed with and without heating of the powder bed. *(Uddin, S.Z., Murr, L.E., Terrazas, C.A., Morton, P., Roberson, D.A., Wicker, R.B., 2018. Addit. Manuf. 22, 405. With kind permission of Elsevier.)*

PROCESSOS DE MANUFATURA ADITIVA

DIRECTED ENERGY DEPOSITION – Material obtido

Material Al 6061 - PBF

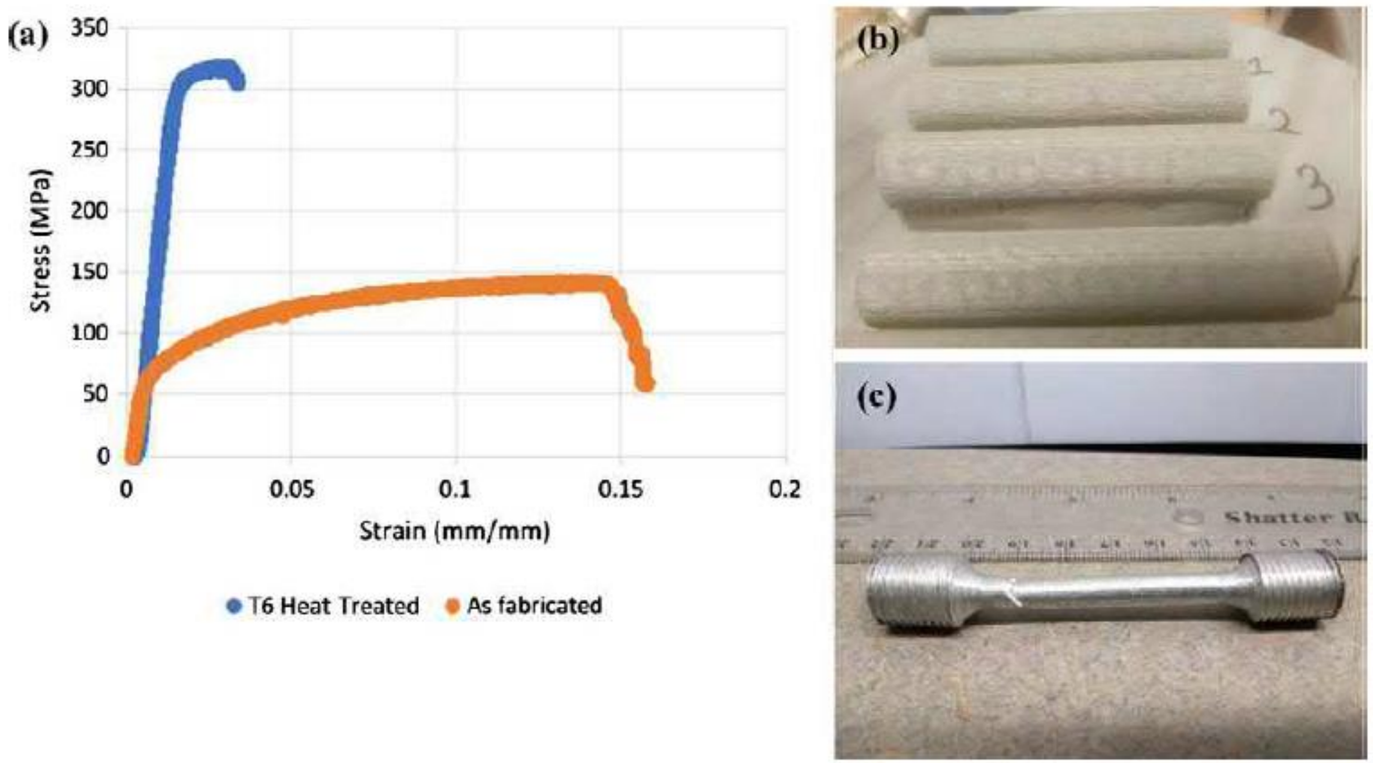

Fig. 3.10 (a) Representative stress-strain diagram of LPBF fabricated AA6061 specimens as fabricated and T6 heat treated. (b) Solid cylinders built in *X*-direction and still on build plate; tensile specimens were machined out of these cylinders. (c) LPBF fabricated AA6061 tensile testing specimen after fractured. *(Uddin, S.Z., Murr, L.E., Terrazas, C.A., Morton, P., Roberson, D.A., Wicker, R.B., 2018. Addit. Manuf. 22, 405. With kind permission of Elsevier.)*

DIRECTED ENERGY DEPOSITION – Material obtido

Material Al 6061

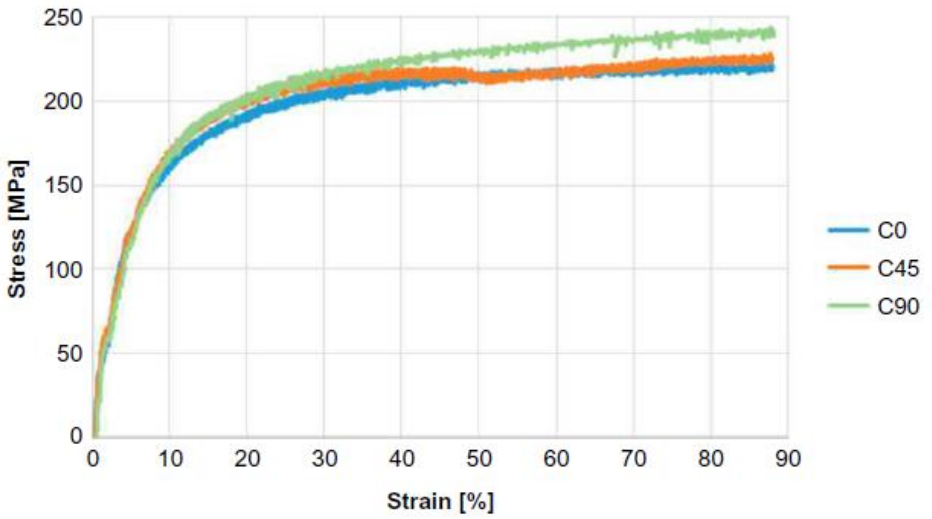

Fig. 3.48 Compressive stress-strain plot for AA6061. *(Rønneberg, T., 2016. Characterization of Aluminium Components Produced by Additive Manufacturing. Norwegian University of Science and Technology, Trondheim. With kind permission of Dr. Tobias Rønneberg.)*

(a) C0. (b) C45. (c) C90.

Fig. 3.49 AA6061 specimen after compression testing. (a) C0, (b) C45, and (c) C90. *(Rønneberg, T., 2016. Characterization of Aluminium Components Produced by Additive Manufacturing. Norwegian University of Science and Technology, Trondheim. With kind permission of Dr. Tobias Rønneberg.)*

DIRECTED ENERGY DEPOSITION – Material obtido

Material Inóx

Table 3.9 Summary of mechanical properties of AISI 304, 316, and 316L stainless steels fabricated by additive manufacturing compared with wrought properties reported in the literature.

	Stainless steel alloy	Laser power (W)	Scanning speed (mm/s)	Linear heat input (J/mm)	Density	Orientation	Yield strength (MPa)	Tensile strength (MPa)	Elongation (%)
Directed energy deposition									
Griffith et al. (2000)	304	–	–	–	100%	Longitudinal	448	710	59
						Transverse	324	655	70
Griffith et al. (1996, 2000)	316	–	–	–	100%	Longitudinal	593	807	30
						Transverse	448	793	66
Xue et al. (2010) [57]	316	–	–	–	93.2%–97.4%	Longitudinal	363–487	648–970	20–44
Zhang et al. (2014) [20]	316	600–1400	2–10	75–500	–	Longitudinal	558	639	21
						Transverse	352	536	46
de Lima et al. (2014) [58]	316	200–350	3–8	24–60	91%	Transverse	207–261	414–539	38–45
Yu et al. (2013) [2]	316L	570/750	13/17	45	99.6%	Longitudinal	490	685	51
						Transverse	280	580	62
Ma et al. (2013) [38]	316L	600–1650	7–23	69–90	96.5–97.5%		400–440	430–510	14–20
Wrought									
Guan et al. (2013) [6]	304						≥205	≥520	≥40
Tolosa et al. (2010) [59]	316						220–270	520–680	40–45

–, Unspecified.

Wang, Z., Palmer, T.A., Beese, A.M., 2016. Acta Mater. 110, 226. With kind permission of Elsevier.

DIRECTED ENERGY DEPOSITION – Material obtido

Material Inóx

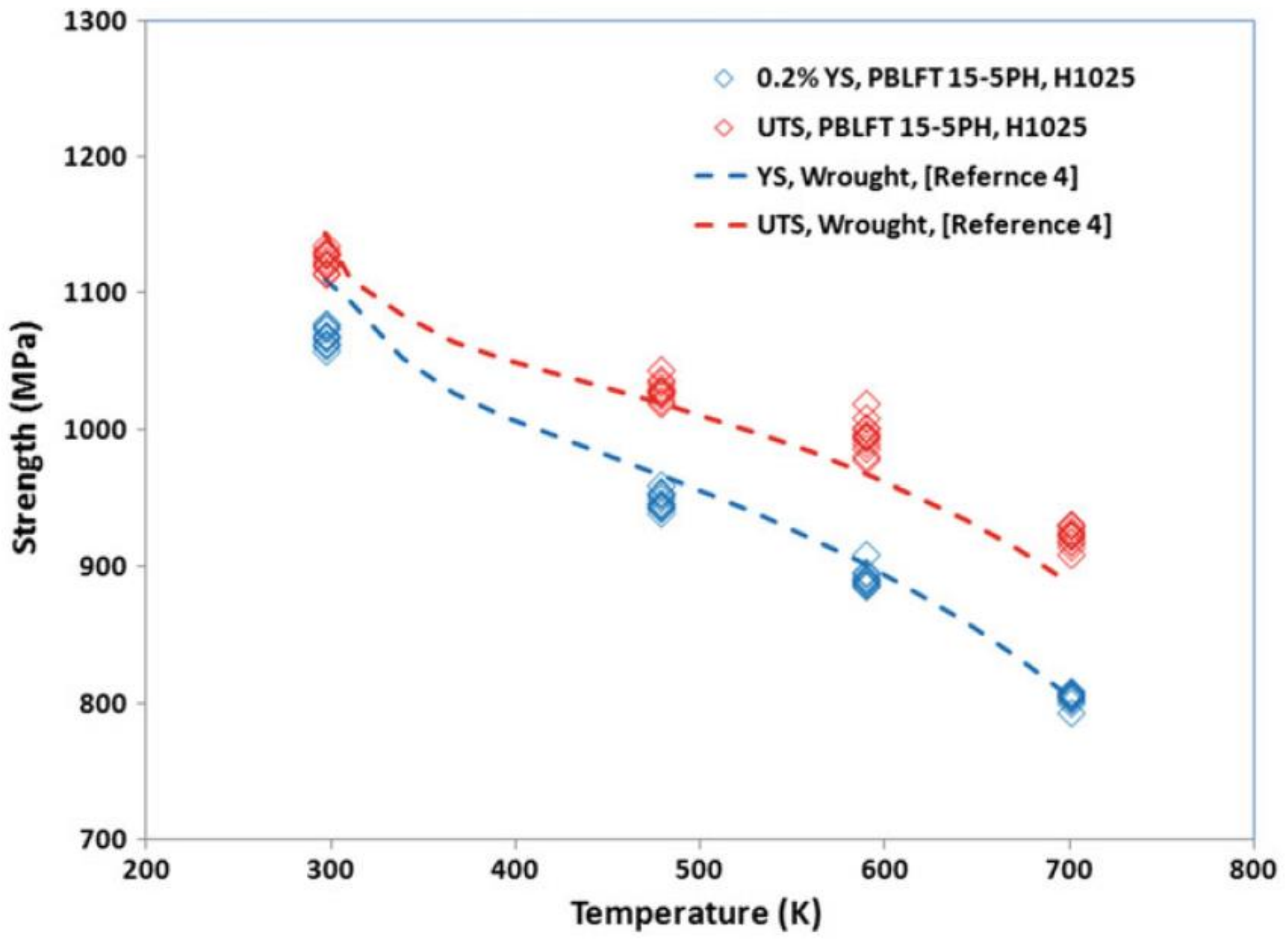

Fig. 3.5 Comparison of tensile strengths of PBLFT 15-5PH to wrought 15-5PH

DIRECTED ENERGY DEPOSITION – Material obtido

Material Inconel 718

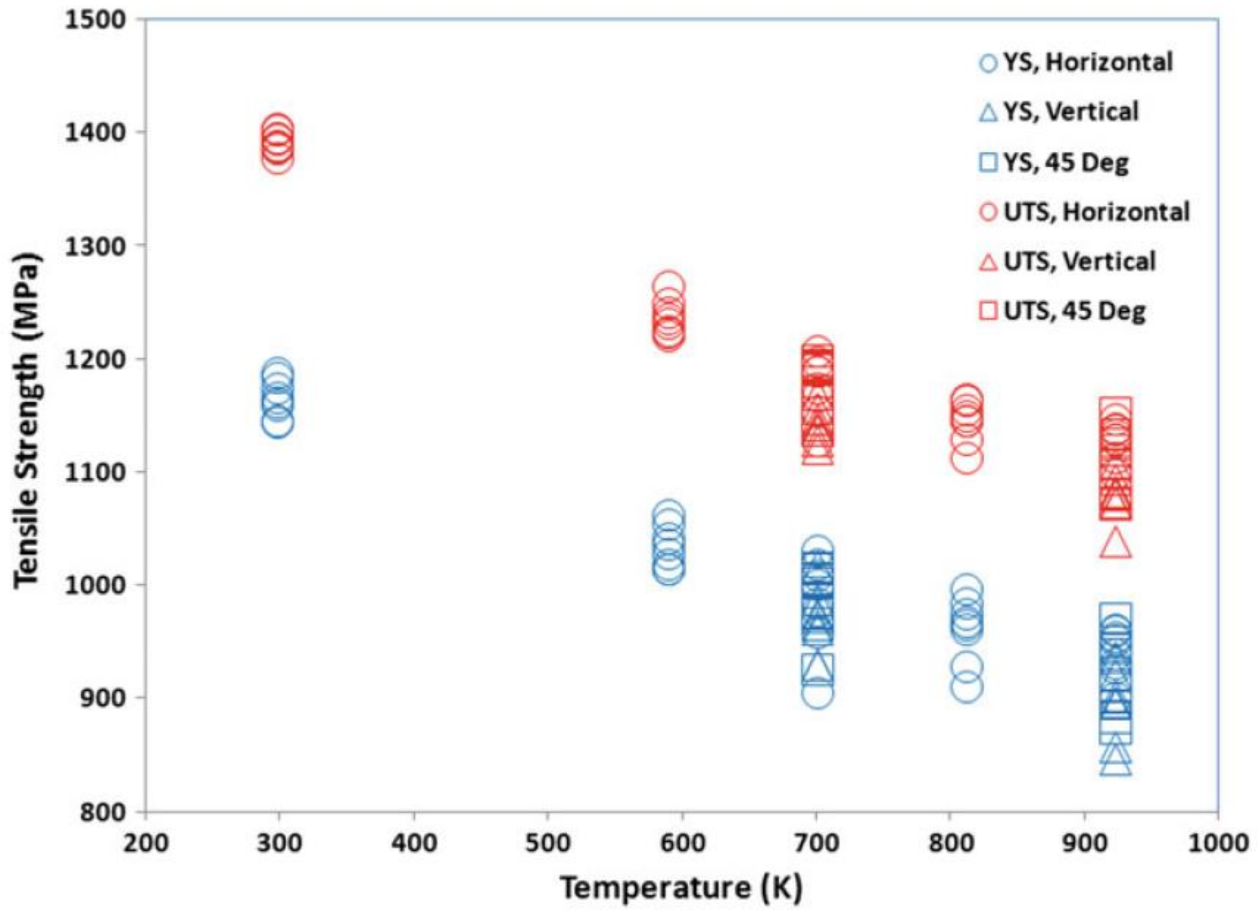

Fig. 3.2 Comparison of Tensile Strengths of PBLFT IN-718 for various build orientations

DIRECTED ENERGY DEPOSITION – Material obtido

Material Inconel 718

Fadiga

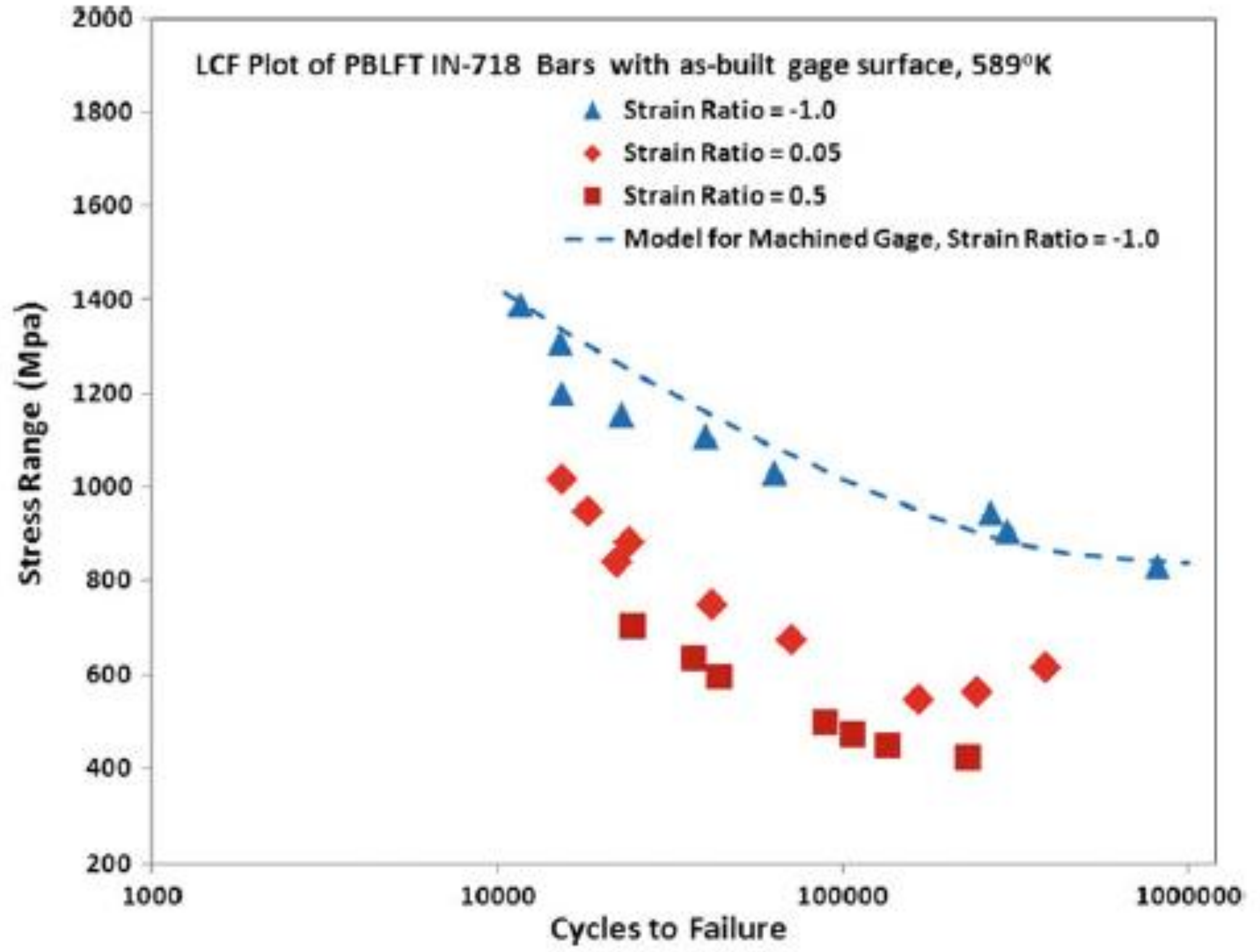

Fig. 3.8 LCF Data at 589 K for PBLFT IN-718 with as-built gage surface, all vertically built bars